



Effects of process parameters on forming force and accuracy in cold roll-beating forming external tooth groove

Long Li¹ · Yan Li¹ · Mingshun Yang¹ · Xudong Xiao¹ · Limu Cui¹ · Fengkui Cui²

Received: 22 May 2018 / Accepted: 3 October 2018 / Published online: 15 October 2018
© Springer-Verlag London Ltd., part of Springer Nature 2018

Abstract

Cold roll-beating forming is an incremental cumulative plastic forming technology that uses rolling wheels to impact and roll a metal target at room temperature. The process parameters of cold roll-beating forming influence the forming process and its accuracy. In this paper, these influences are studied for the case of cold roll-beating forming an external tooth groove. First, the process and characteristics of cold roll-beating forming are analyzed to determine the key process parameters for forming external tooth grooves. Next, forming experiments and finite element simulations are carried out for roll-beating AISI 1045 (DIN C45). The forces, material deformation, and formed surface characteristics are analyzed for the process of cold roll-beating forming of an external tooth groove. Finally, the effects of the roll-beating method, spindle speed, and roll-beating density on the forces, forming defect, angle of the groove profile, and surface roughness are discussed. This study will serve as a reference for reducing forming force, restraining adverse deformation, and controlling forming quality by optimizing process parameters.

Keywords Cold roll-beating · Forming · Tooth groove · Force-accuracy

1 Introduction

Gears, racks, spline shafts, and other functional elements that possess external teeth are widely used in various mechanical products, especially in the automotive industry and the equipment manufacturing industry. With the increasing demand for industrial products, the requirements for performance and accuracy of such parts have also increased. The manufacturing industry is facing new challenges, not only with regard to the increasing production efficiency and improving product performance but also with regard to reducing the consumption of resources [1, 2]. Currently, the external teeth of solid components are mainly produced by two methods: cutting and plastic forming. Plastic forming can directly improve the mechanical properties of products and the material utilization [3]. The

traditional plastic forming method involves rolling, die forging, etc. [4], the equipment for which requires a relatively high forming force and high energy consumption of forming equipment. To reduce the forming force and energy consumption, forming methods utilizing incremental processes have been developed [5, 6], such as flow forming methods for forming high-quality internal teeth [7] and external teeth [8] or orbital forming method for forming ring gears [9] and bevel gears [10].

Cold roll-beating forming technology is an incremental cumulative plastic forming technology that uses a rolling wheel to impact and roll metal at room temperature [11]. However, unlike the aforementioned incremental forming technology, the cold roll-beating forming process does not require heating, which reduces energy consumption. In addition, the surface of the formed parts does not require subsequent modification or finishing. Thus, the production process chain is short, and the production efficiency is higher. Meanwhile the forming process requires no additional die, which allows it to have higher production flexibility [12, 13]. This technology was first proposed by Ernst Grob, who applied for patent for related devices [14]. However, there was minimal subsequent research on the topic.

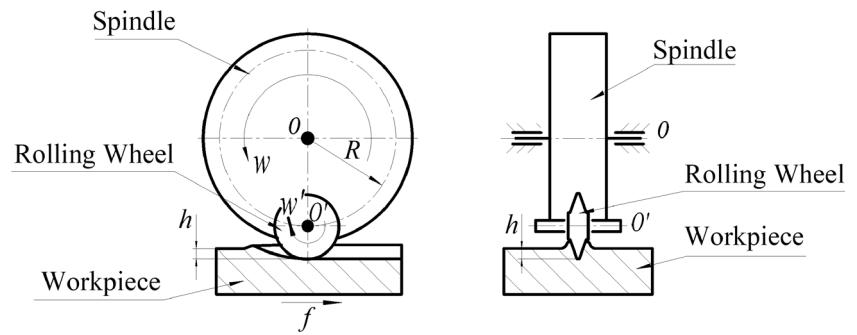
In recent years, the cold roll-beating forming process has been investigated using numerical simulation. Cui et al. [12]

✉ Yan Li
jyxy-ly@xaut.edu.cn

¹ School of Mechanical and Precision Instrument Engineering, Xi'an University of Technology, No.5 South Jinhua Road, Xi'an 710048, Shaanxi, China

² School of Mechatronics Engineering, Henan University of Science and Technology, Luoyang 471003, Henan, China

Fig. 1 Principle diagram of cold roll-beating forming



established a simplified finite element model of the involute spline cold roll-beating forming process, analyzed the deformation behavior of metal in the forming process, summarized the deformation characteristics of different regions, and qualitatively described the formation of the metal fibrous grain structure in the forming process. In addition, Cui et al. [15] employed the finite element software DEFORM-3D to analyze the cold roll-beating forming of a ball screw and provided a preliminary description of the influence of roll-beating speed and feed transmission ratio. Li et al. [16, 17] established a model of the cold roll-beating forming of an aluminum rack using ABAQUS and analyzed the stress, strain, and forming force of the forming process of the different cold roll-beating methods. It was concluded that loading is fast and unloading is slow when the workpiece is fed against the direction of spindle rotation. The stress and strain of different cold roll-beating methods are similar. In these studies, to reduce computational cost, only one or a limited number of roll-beating processes were calculated, which led to the calculation results reflecting only the forming force and metal deformation of a small region. Meanwhile, only single process parameter or a small range of process parameters has been studied, and there has been no further discussion or experimental research. It is difficult to characterize the relationship between the formation process parameters and the forming force or forming quality of the entire forming process.

Some scholars have studied cold roll-beating forming through kinematic modeling and experimental methods. Based on the kinematic and geometric relationships of the cold roll-beating forming process, Cui et al. [18] provided a mathematical model of the kinematic relationship of cold roll-beating forming screw and analyzed the cause of forming errors of the ball screw grooves. Under the ideal conditions for cold roll-beating forming, Yang et al. [19] derived a simplified mathematical model of the scallop height of the bottom of a tooth, without considering the influence of dynamics. To a certain extent, the cause of the ripples of the tooth bottom was

explained, and the influence of the process parameters on the tooth bottom scallop height was analyzed. These studies made many assumptions and simplifications of the actual deformation process of metal. Thus, the calculated error values are larger. Performing a statistical analysis of the experimental results, Cui et al. [20] established a multiple regression model of the relationship between the surface residual stress of a cold roll-beating spline and the process parameters. The results of the prediction results were demonstrated to be reliable for a certain range of parameters.

The research on the cold roll-beating forming process has mostly focused on analysis and discussion of several process parameters for a single target. There is a lack of comprehensive research on forming force, dimension accuracy, and surface quality of cold roll-beating forming under the combined effect of multiple process parameters. Therefore, in this paper, the effects of process parameters on the forming of external tooth groove cold roll-beating forming are studied. First, the principle behind cold roll-beating forming is introduced, and the key process parameters affecting the forming process are selected, as they pertain to the technological characteristics of cold roll-beating forming external teeth of functional elements. Then, experimental equipment and finite element models of an external tooth groove by cold roll-beating forming are established. Next, experiments and the finite element method (FEM) are combined, and the characteristics of forming force, deformation, and formed surface are analyzed. Then, the physical parameters for evaluating forming force, deformation, and formed surface are given. Finally, the influence of key process parameters on the forming force, dimensional accuracy, and surface quality is obtained by experiment and discussed.

2 Cold roll-beating forming process

The basic principle of cold roll-beating forming is shown in Fig. 1. A rolling wheel with a designated tooth profile is

Table 1 Chemical composition (wt%) of AISI 1045

Element	C	Mn	Si	S	P	Cr	Ni
wt%	0.44~0.50	0.51~0.73	0.29~0.35	0.04	0.03~0.04	0.16~0.18	0.12~0.22

Table 2 Mechanical properties of AISI 1045

Projects	Parameter value
Density (kg/m ³)	7810
Elasticity modulus (GPa)	201
Poisson ratio	0.269
A (MPa)	525.4
B (MPa)	541.625
<i>n</i>	0.4296
<i>C</i>	0.0212
ϵ'_{0}	0.008

assembled eccentrically on the spindle. Then, the spindle rotates at a speed w and drives the rolling wheel. The center of spindle rotation is O and the revolution radius of the rolling wheel is R . The rolling wheel rotates under the effect of friction when it roll-beats the workpiece. The rotation center of the rolling wheel is O' . During each rotation of the spindle, the rolling wheel roll-beats the workpiece once. The depth of roll-beating is determined by the desired shape of the tooth. During the forming process, the workpiece is continuously fed at a speed f such the plastic deformation caused by each beating gradually accumulates. Then, the shape of the required tooth groove profile is eventually formed. A variety of parts, such as lead screws, external splines, external gears, racks, and other functional elements with external teeth [12, 16, 18, 21], can be formed by varying the rotation and feed motion of the workpiece. Although the types of formed parts are different, the single tooth groove forming process for all parts is shown in Fig. 1. The spindle rotation and the workpiece feed are the most basic

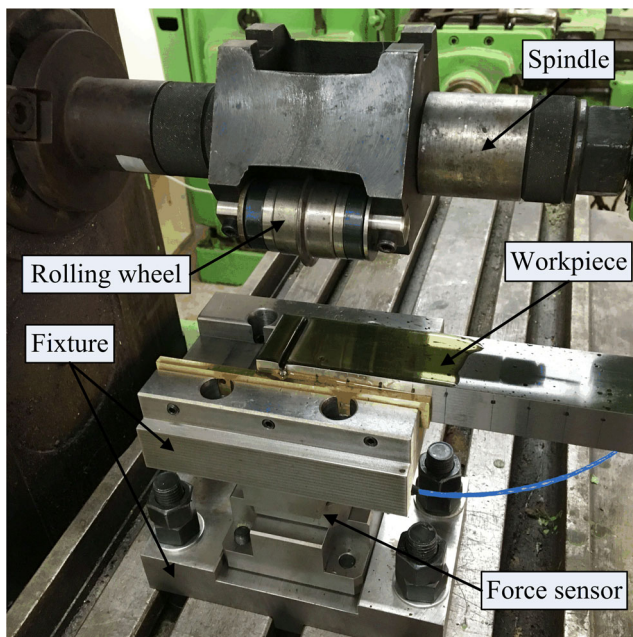


Fig. 2 Cold roll-beating experimental device

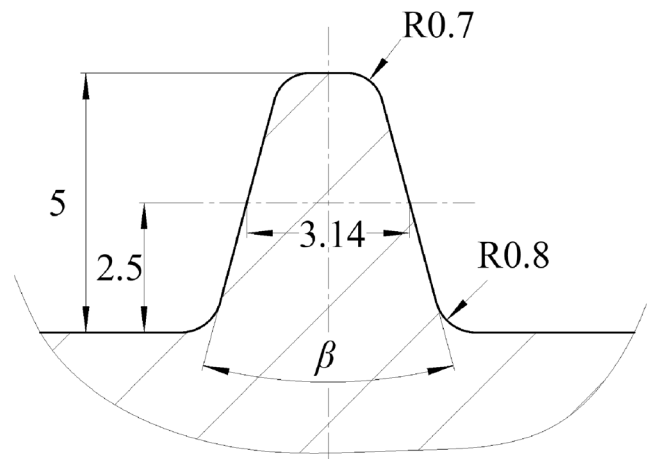


Fig. 3 Tooth section of the rolling wheel

movements of cold roll-beating forming, of which direction and speed directly affect the forming process.

Similar to milling, the roll-beating method can be defined as down-beating and up-beating according to the relationship between the tangential direction of the rotation of the spindle and the workpiece feed direction. When the rolling wheel roll-beats the workpiece, during down-beating, the workpiece is consistently fed at the tangential velocity of the rotating spindle, as shown in Fig. 1. If the feed direction of the workpiece is opposite the tangent direction of the rotating spindle, then it is considered up-beating. Similar to the down-milling and up-milling, differences in the roll-beating method can affect the loading of the workpiece and the deformation of the metal. Therefore, the selection of roll-beating method must be considered.

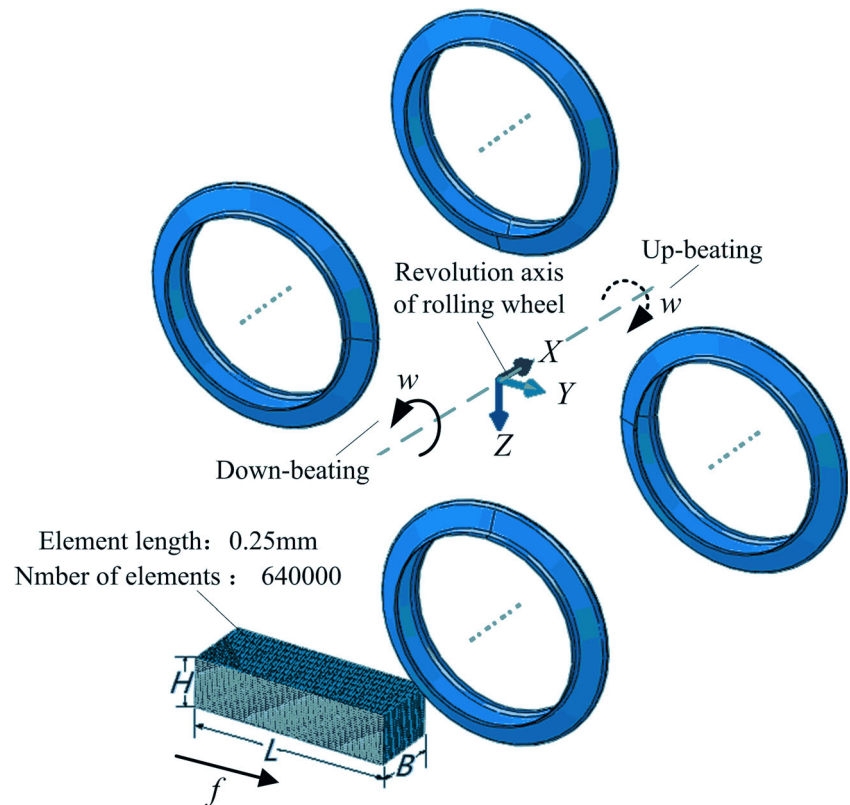
According to the cold roll-beating forming principle, the spindle speed directly affects the impact speed of roll-beating. This parameter determines the strain rate of the metal deformation during the forming of metal. The feed speed is a measure of forming efficiency. The ratio of feed speed to spindle speed is known as the roll-beating density—that is, the number of roll-beats per unit length—which reflects the amount of metal involved in the deformation of each roll-beating.

The basic model of cold roll-beating for forming the external teeth of functional elements is shown in Fig. 1. This paper

Table 3 Selection of process parameter

Parameter	Method	Spindle speed, w (r/min)	Feed, f (mm/min)
Levels	Down-beating	475	30
			60
			120
	Up-beating	950	240
			480
		1500	960

Fig. 4 Finite element model of cold roll-beating forming



will mainly discuss the combined influence of the roll-beating method, the spindle speed, and the roll-beating density on the forming force, the forming precision, and the surface quality.

3 Methodologies

3.1 Experimental material and properties

In this paper, AISI 1045 (DIN C45, tempered steel) is used as the cold roll-beating forming workpiece material. This is a common medium-carbon steel with good mechanical properties that, after proper heat treatment, can acquire a certain toughness and wear resistance. Because of this ability, the steel is widely used in the manufacture of various important

structures and transmission parts. The chemical composition of the material used in this paper is shown in Table 1.

Based on the principle of cold roll-beating forming, the relevant characteristics of materials are the local compression load and work hardening. Therefore, it is necessary to consider the effects of strain rate and hardening when describing the constitutive relations of the material. Among commonly used constitutive models, the Johnson-Cook (J-C) model is an empirical viscoplastic constitutive equation that can describe the effects of strain rate and hardening on metal materials. In this paper, the J-C constitutive equation is used to describe the constitutive relation of the workpiece material. During each roll-beating process, the contact area and contact time of the rolling wheel rolling over the workpiece are short. Thus, the heat generated by deformation and friction is small and is

Fig. 5 Force of the workpiece with down-beating: **a** z-direction force and **b** y-direction force

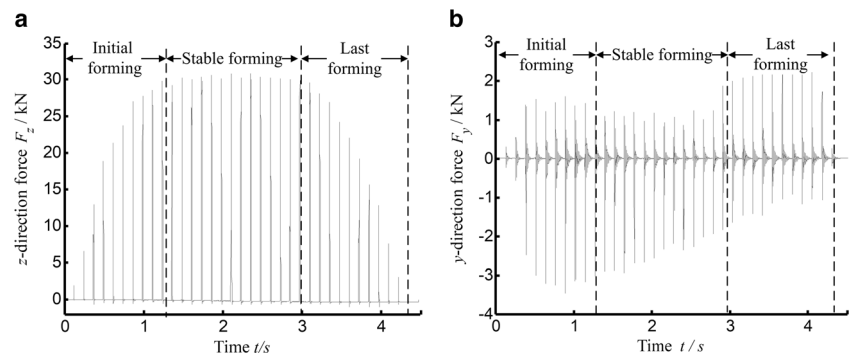
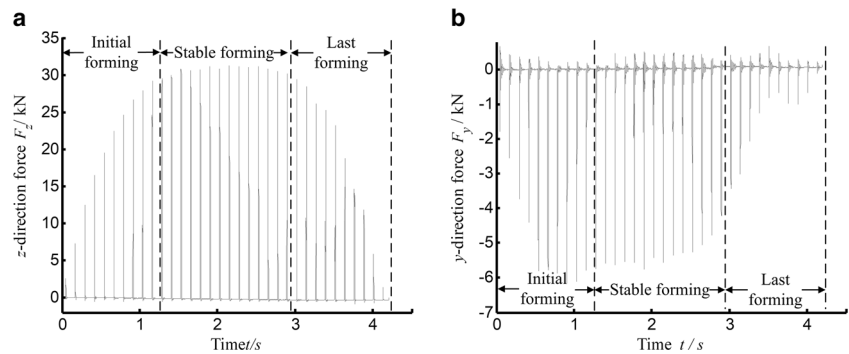


Fig. 6 Force of the workpiece with up-beating: **a** z-direction force and **b** y-direction force



quickly transferred to the workpiece. At the same time, because the cold roll-beating forming process is an intermittent forming process, the workpiece and the rolling wheel can dissipate heat during each roll-beating process. The effect of temperature generated during the forming process can be neglected. The mathematical expression of the J-C constitutive model used in this paper is shown in Eq. (1) as follows:

$$\sigma = [A + B\varepsilon^n] \times \left[1 + C \ln\left(\frac{\dot{\varepsilon}'}{\dot{\varepsilon}'_0}\right) \right] \tag{1}$$

where σ is the equivalent flow stress; A is the yield limit; B is the hardening modulus; n is the hardening coefficient; ε is the strain; C is the strain rate constant; m is the thermal softening coefficient; $\dot{\varepsilon}'$ is the equivalent plastic strain rate; and $\dot{\varepsilon}'_0$ is the strain rate reference.

The parameters of the J-C constitutive model of the material were obtained by a static compression experiment and a separate Hopkinson pressure bar experiment. The above parameters and other mechanical properties are summarized in Table 2.

3.2 Experimental device and parameters

As shown in Fig. 2, cold roll-beating experiments were carried out on a reformed horizontal milling machine. The rolling wheel was made of 20CrMnTi, underwent carburizing modulation treatment, and had a surface hardness 58–64 HRC and a surface roughness Ra 0.2~0.4. The rotation radius of the top of the tooth and the revolution radius of the rolling wheel were

24 mm and 72 mm, respectively. A piezoelectric three-direction force sensor PCB261A03 (PCB®) was installed under the workpiece by the fixture. The workpiece was coated with L-CKC100 (SINOPEC®) gear oil during forming.

The workpiece was 40 mm in length (along the feed direction) and 20 mm thick. The dimension of the profile of the rolling wheel tooth is shown in Fig. 3. The angle of the tooth profile of the rolling wheel was β , which was measured and found to be 31.1°.

The forming depth was 2.5 mm, and the remaining process parameters are shown in Table 3. A total of 36 groups of experiments were conducted at a variety of process parameters.

A VHX-5000 3D microscope system (Keyence®) was used to measure the geometrical dimensions of the formed tooth profile. The formed workpiece was cut, and the surface morphology of the tooth groove wall was measured by a DCM 3D laser confocal microscopy (Leica®).

3.3 Finite element modeling

Based on the experiment, a computational model was established in the finite element software ABAQUS, as shown in Fig. 4. The workpiece is fed along the y -direction, and the rolling wheel axis of revolution is x . The length, width, and height of the model workpiece are calculated to be 40 mm, 25 mm, and 10 mm, respectively. The friction coefficient is 0.05, based on the value used for common metal cold-rolling forming [22]. Using the C3D8R element to structure the mesh workpiece, 161, 101, and 41 nodes are distributed along L , B ,

Fig. 7 Forces of the workpiece during the roll-beating: **a** down-beating and **b** up-beating

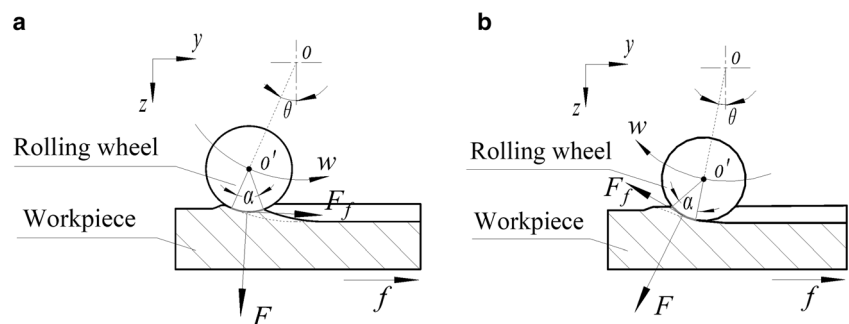
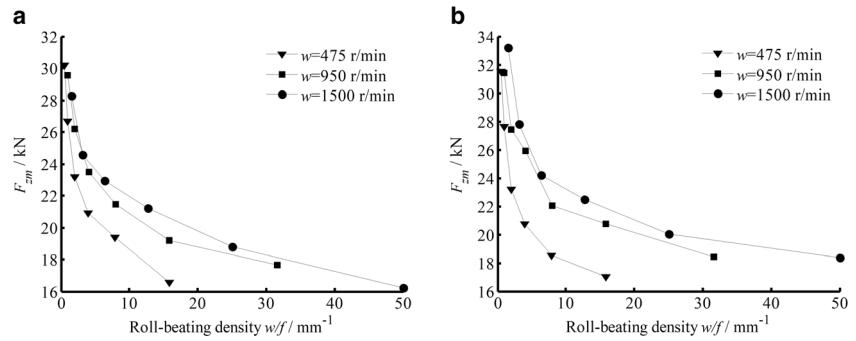


Fig. 8 The F_{zm} under the different process parameters: **a** down-beating and **b** up-beating



and H , respectively. The total number of elements is 640,000. ALE adaptive meshing is used in the calculation.

To improve the efficiency of calculation, the computational model distributes four rolling wheels along the rotational axis of the spindle. Compared to the single rolling wheel in the experiment, the speed of the workpiece in this model can be increased by four times as long as the spindle speed and roll-beating density are identical to those of the experiment. The rolling wheels are treated as an analytic rigid body. Elastic deformation of the rolling wheel and the dynamic characteristics of the process system are ignored.

4 Results and discussion

4.1 Roll-beating force

The three-direction force sensor is used to measure the x , y , and z components of the forces to which the workpiece is subjected at different combinations of process parameters. These coordinates are consistent with the FEM. The z -direction is perpendicular to the surface of the workpiece to be formed and points toward the interior of the workpiece. The y -direction is aligned with the feed direction. Due to the geometric symmetry of the formed tooth shape, the forming force is balance in the x -direction. Then, from the forming principle, it is known that the force F_z in the z -direction is the primary force responsible for plastic deformation of the metal and that the force F_y in the y -direction directly affects the feed and

forming quality of the workpiece. Consequently, we focus on F_z and F_y .

Figures 5 and 6 show the changes of F_z and F_y , respectively, that result from down-beating and up-beating during the experiment when the spindle speed is 475 r/min and the feed speed is 960 mm/min.

The variation in F_z during down-beating is similar to that of up-beating, as shown by Fig. 5a and Fig. 6a. At the beginning of forming process, the peak value of F_z of each roll-beating increases gradually with each roll-beating, which is the initial forming stage. The peak value of F_z of each roll-beating tends to be stable and attains the maximum value during the forming process; this is defined as the stable forming stage. Later in the forming process, the peak value of F_z of each roll-beating gradually decreases, representing the last forming stage.

The variation of F_y is different during down-beating and up-beating. As shown in Fig. 5b, for down-beating, the direction of F_y changes during each roll-beating. In the initial forming stage, the force opposite the feed direction is larger, and its peak value increases gradually until reaching the maximum value it will attain over the course of the forming process. In the stable forming stage, the effect of the force opposite the feed direction gradually decreases. In the last forming stage, the workpiece is subjected to larger forces in the feed direction, and the peak value of F_y of each roll-beating reaches a maximum. As shown in Fig. 6b, for up-beating, the direction of F_y is always opposite the feed direction. The peak value of F_y of each roll-beating increases rapidly during the initial forming stage and reaches a maximum before the stable forming stage, after which it decreases and remains constant

Fig. 9 The F_{ym} under the different process parameters: **a** down-beating and **b** up-beating

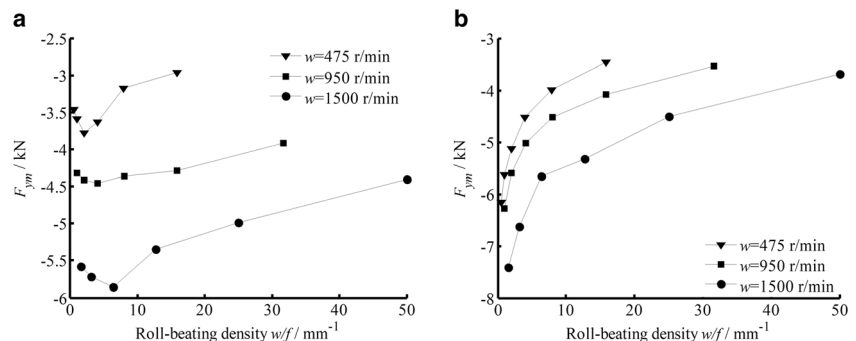


Fig. 10 Formed tooth groove of experiment: **a** $w = 475$ r/min, **b** $w = 950$ r/min, and **c** $w = 1500$ r/min



in the stable forming stage. Finally, the value decreases in the last forming stage.

Forces analysis diagrams of workpiece for different roll-beating method are shown in Fig. 7, in which the reasons for the variation of F_z and F_y can be better understood. α is the center angle of the contact arc of the rolling wheel and the workpiece, and θ is the swing angle of the rolling wheel during the roll-beating process.

The forming force F and friction force F_f of the workpiece are decomposed into the z - and y -directions. For down-beating, F_y and F_z can be calculated as follows:

$$F_z = F \cos\left(\theta - \frac{\alpha}{2}\right) + F_f \sin\left(\theta - \frac{\alpha}{2}\right) \tag{2}$$

$$F_y = F_f \cos\left(\theta - \frac{\alpha}{2}\right) - F \sin\left(\theta - \frac{\alpha}{2}\right) \tag{3}$$

For up-beating, F_y and F_z can be expressed as:

$$F_z = F \cos\left(\theta + \frac{\alpha}{2}\right) - F_f \sin\left(\theta + \frac{\alpha}{2}\right) \tag{4}$$

$$F_y = -\left(F_f \cos\left(\theta + \frac{\alpha}{2}\right) + F \sin\left(\theta + \frac{\alpha}{2}\right)\right) \tag{5}$$

where the negative value of F_y indicates that the direction of F_y is opposite the feed.

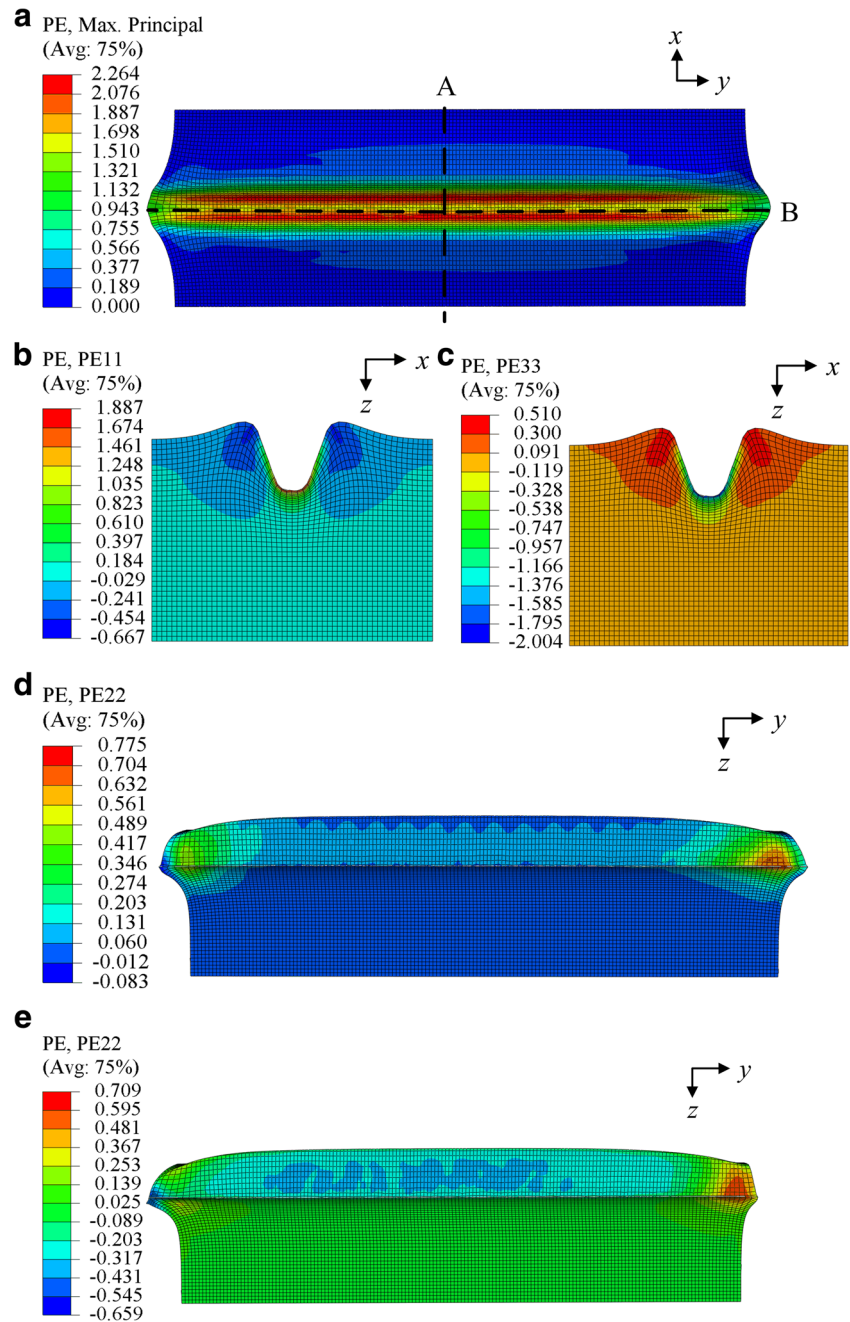
The contact area between the roller and the workpiece during metal forming is defined as S , and the friction coefficient is μ . Then, the forming force F and the friction force F_f can be expressed as:

$$\begin{cases} F = \sigma S \\ F_f = \mu F \end{cases} \tag{6}$$

The rolling wheel rotates during the forming process. Thus, both rolling friction and sliding friction exist between the rolling wheel and the workpiece. Referring to the friction coefficient of other similar forming methods [22–24] and considering the lubricating oil used in the forming process, we believe that the friction coefficient μ is smaller in cold roll-beating forming. Therefore, F_f is much smaller than F , and the ranges of θ and α are also small. So Eqs. (2) and (4) show that F_z is close to F for down-beating and up-beating. From Eq. (6), it can be observed that, during the forming process, F is mainly affected by S under given the forming conditions. In the initial forming stage, the maximum value of S gradually increases with each roll-beating. In the stable forming stage, the rolling wheel reaches its maximum forming depth, and the maximum value of S no longer changes with each roll-beating. In the last forming stage, the workpiece gradually away from the rolling wheel, and the maximum value of S gradually decreases with each roll-beating. Therefore, the peak value of F_z during each roll-beating increases gradually in the initial forming stage, remains constant in the stable forming stage, and decreases gradually in the last forming stage, as shown in Fig. 5a and Fig. 6a.

For F_y under the effect of down-beating, Eq. (3) shows that the direction of F_y depends on θ and $\alpha/2$. When $\tan(\theta - \alpha/2)$ is greater than μ , F_y is negative. F_y coincides with the feed direction when $\tan(\theta - \alpha/2)$ is less than μ . Therefore, under the effect of down-beating, the variation of F_y is complex, as shown in Fig. 5b. However, under the effect of up-beating, Eq. (5) shows that the y components of F and F_f are always negative, which means that the direction of F_y is always opposite the feed direction, and that it follows a trend similar to that of F_z , as shown in Fig. 6.

Fig. 11 Plastic strain of the material: **a** principal plastic strain, **b** x-direction plastic strain on A cross-section, **c** z-direction plastic strain on A cross-section, **d** y-direction plastic strain on B cross-section with down-beating, and **e** y-direction plastic strain on B cross-section with up-beating



The average peak of F_z in the stable forming stage is defined as F_{zm} , and the maximum value of F_y in the forming process is F_{ym} . Figures 8 and 9 show F_{zm} and F_{ym} for the different roll-beating methods, spindle speed, and roll-beating densities.

As shown in Fig. 8, when the spindle speed and roll-beating density are the same, F_{zm} during up-beating is higher than during down-beating, an effect that is more obvious when the roll-beating density is small. This is mainly due to the relative relationship of the motion of down-beating between the rolling wheel and the workpiece, which makes the contact arc between the rolling wheel and the workpiece smooth and the contact area smaller than during up-beating. During down-

beating the rolling, wheel first beats the material that has not been deformed, and work hardening of this portion of the material is weaker. In contrast, the metal surface that is rolled during up-beating is subjected to plastic deformation many times before it is deformed again, and the hardening is more obvious.

For F_{ym} , in addition to the above factors, the inconsistency of the directions of the tangential forces in the down-beating process should also be taken into account, so F_{ym} of up-beating under the same conditions is also larger than that of down-beating. This effect becomes more significant when the roll-beating density is small, as shown in Fig. 9.

Fig. 12 Metallographic experiment: **a** metallographic sample of the tooth groove in the stable forming stage, **b** metallographic structure of position 1, **c** metallographic structure of position 2, and **d** metallographic structure of position 3

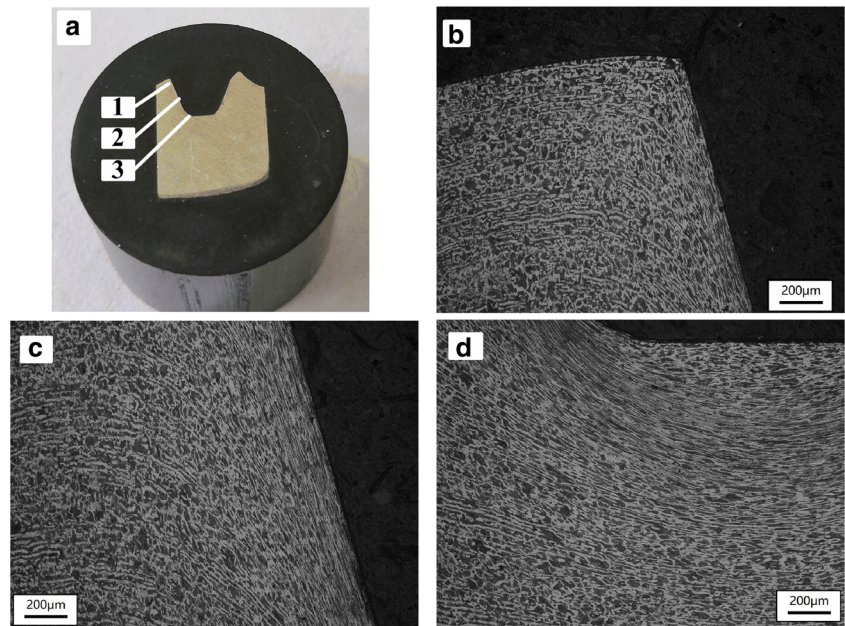


Figure 8 shows that, regardless of the roll-beating method, F_{zm} decreases as the roll-beating density increases due to the decrease in the amount of deformation produced by each roll-beating on the metal. After the roll-beating density exceeds 10 mm^{-1} , this decrease tends to plateau.

As shown in Fig. 9, for up-beating, the relationship of F_{ym} with roll-beating density is the same as that of F_{zm} . For down-beating, as the roll-beating density increases, F_{ym} first increases and then decreases. When the spindle speed is 475 r/min, 950 r/min, and 1500 r/min, and the roll-beating density is approximately 2 mm^{-1} , 4 mm^{-1} , and 6 mm^{-1} , respectively, F_{ym} attains a maximum.

For the same roll-beating method and roll-beating density, the increased spindle speed will increase the strain rate of metal forming, and the flow stress σ of AISI 1045 increases with the increase in the strain rate. Thus, the forming force of the workpiece increases. According to the J-C constitutive model, for the AISI 1045, the effect of strain rate on flow stress σ weakens gradually with the increase in the strain rate. Therefore, F_{zm} and F_{ym} increase as the spindle speed

increases. The larger the spindle speed is, the smaller the increase, as shown in Figs. 8 and 9.

4.2 Deformation

The tooth grooves obtained from the cold roll forming experiment are shown in Fig. 10. Each tooth groove is formed from the lower end, and the feed speed increases gradually from left to right. The first six tooth grooves are formed by down-beating, and the latter six are formed by up-beating. The experimental results show that the middle part of the formed tooth groove (which is in the stable forming stage) exhibits good consistency with regard to the shape and that insufficient metal uplift at both ends of workpiece causes the tooth groove to be shallower. At the same time, in the initial and last forming, apparent metal overflow toward the outside of the workpiece results in a flash similar to that generated by die forging. In addition, the flashes of the initial forming side are shorter when up-beating is utilized.

Fig. 13 Flash length under the down-beating: **a** initial forming side and **b** end forming side

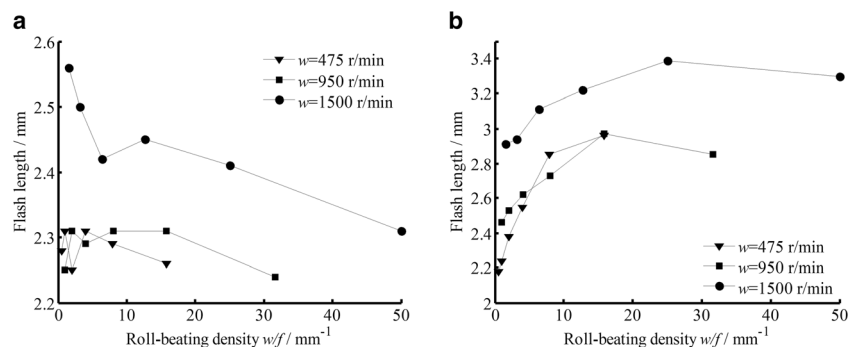
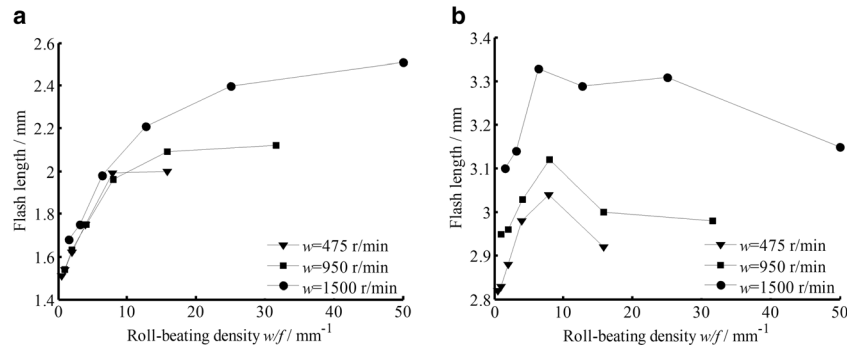


Fig. 14 Flash length under the up-beating: **a** initial forming side and **b** end forming side



To explain the metal deformation characteristics of cold roll-beating forming, the metal deformation during cold roll-beating forming is simulated by the FEM. The results show that the deformation characteristics of the middle part of the tooth groove formed under different process parameters are consistent. The true plastic strain of the material with a spindle speed of 475 r/min, a feed speed of 960 mm/min, and use of down-beating is shown in Fig. 11a–d. The results indicate that the plastic deformation of the middle part of the formed tooth groove is mainly concentrated in the surface layer of the workpiece and that material deformation is largest in the transition zone from the bottom of the tooth groove to the tooth groove wall. The compressed metal mainly extends along the wall of the tooth groove, and the deformation along the y -direction (feed

direction) is very small. At the initial and last stages of forming, the metal deformation along the y -direction is evident, and it causes obvious flash. Figure 11e shows the results of the simulation of up-beating at the same speed and feed rate. Comparing these with the results in Fig. 11d, it can be seen that up-beating inhibits the formation of flash of the initial forming side.

The metallographic structure of the middle part of the tooth groove also indicates that the metal-plastic deformation occurs mainly in the surface layer of the wall of tooth groove and tooth bottom, as shown in Fig. 12. Further, it can be seen that, in the surface layer of the tooth groove, the grain size is finer and the grain structure of the metal is fibrous. To a certain extent, this metallographic observation matches the metal deformation results from the simulation.

Fig. 15 Tooth profile of the rolling wheel and tooth groove profile of stable forming stage

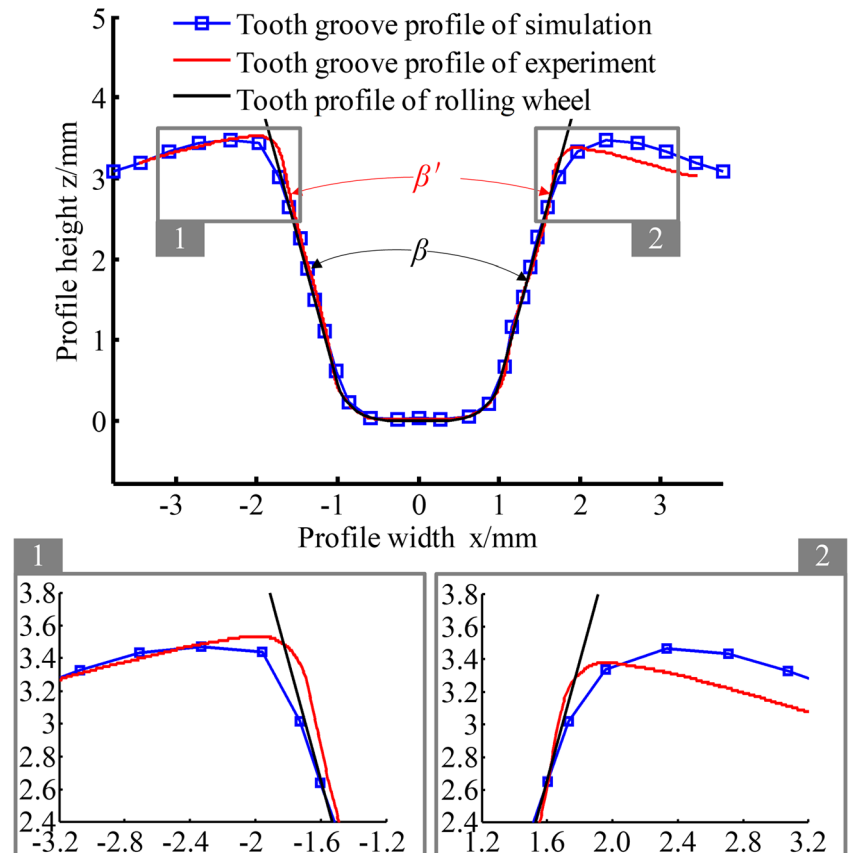
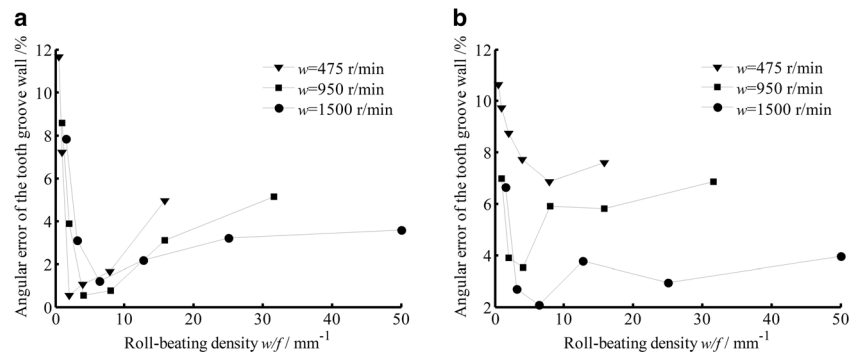


Fig. 16 The effects of process parameters on angular error of the tooth groove wall: **a** down-beating and **b** up-beating



The flash length of the initial and end forming side at different spindle speeds, roll-beating densities, and roll-beating methods was measured. As shown in Figs. 13 and 14, the results indicate that, under the same forming parameters, the flash at the end forming side is longer.

For down-beating, Fig. 13 shows that the flash length of the spindle at 475 r/min and 950 r/min is similar. When the spindle speed is 1500 r/min, the flash length clearly increases. As the roll-beating density increases, the flash length of the initial forming side slightly decreases, and the flash length of the end forming side increases gradually and then stabilizes when the roll-beating density exceeds 10 mm^{-1} .

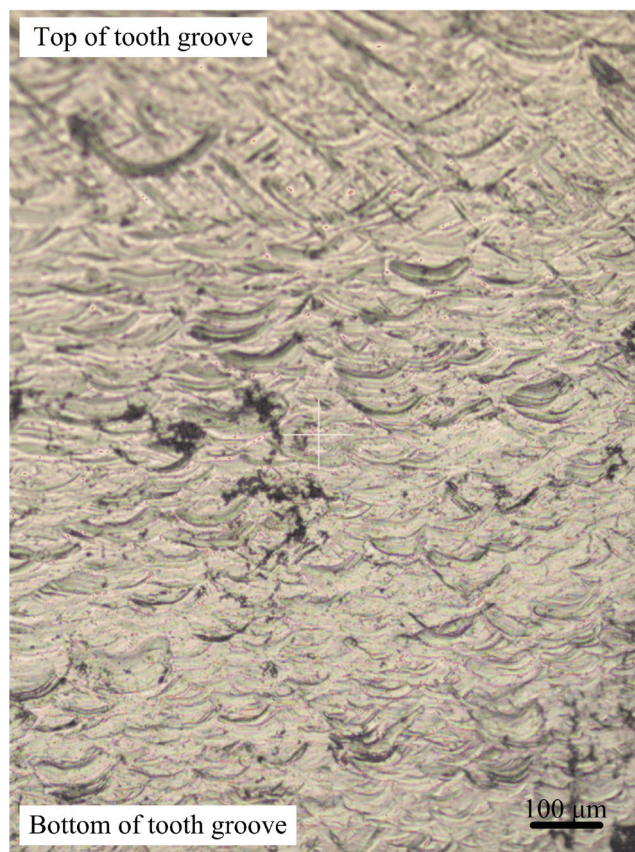


Fig. 17 Surface morphology of tooth groove wall

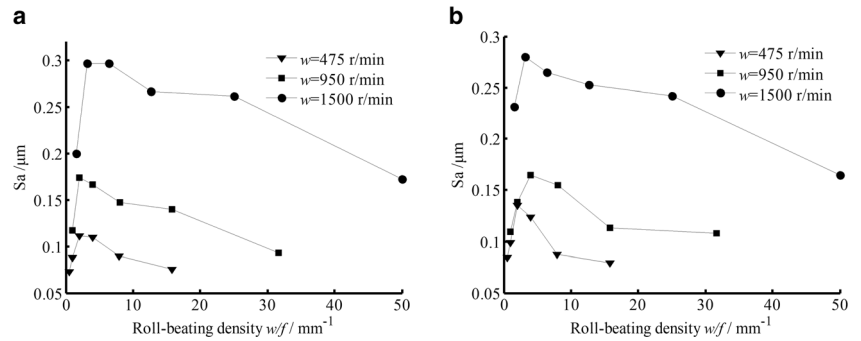
For up-beating, Fig. 14a indicates that, at the same spindle speed, the flash length of the initial forming side increases as the roll-beating density increases, a trend that slows after the roll-beating density exceeds 10 mm^{-1} . When the roll-beating density is less than 10 mm^{-1} , the spindle speed has minimal effect on the flash length of the initial forming side. When the roll-beating density is further increased, the flash length of the initial forming side increases with the spindle speed. Figure 14b shows that the flash length of the end forming side increases obviously as the spindle speed increases and achieves a maximum when the roll-beating density is approximately 10 mm^{-1} at the same spindle speed.

Figure 15 shows the tooth profile of the rolling wheel and the tooth groove profile of the simulation and the experiment during the stable forming stage with a spindle speed of 475 r/min, a feed speed of 960 mm/min, and the use of down-beating. In Fig. 15, β' is the angle of the groove wall. Comparing the results of the simulation and the experiment, the profile from the experiment is seen to be asymmetrical on both sides of the top of the formed groove. The metal bulge on the left side is higher than that on the right. The reason for this asymmetry is assembly error of the rolling wheel and workpiece, and a small amount of deformation of the forming process system, which results in the geometric center line of symmetry of the rolling wheel profile being not perfectly perpendicular to the surface of the workpiece. With the exception of the local asymmetry of the tooth groove top, the error between the simulation results and the experimental results is small, which verifies the simulation result. Figure 15 shows that the profile of the tooth groove obtained by cold roll forming is close to the tooth profile of the rolling wheel. However, because the workpiece exhibits a certain elastic recovery during the forming process, the experimental value of β' is smaller than the value of β of the rolling wheel.

β' was measured with different parameters, and the results show that β' is always smaller than β . The relative error of β' to β is defined as the angular error of the tooth groove wall. The angular errors of the tooth groove wall with different process parameters are shown in Fig. 16.

For down-beating, the spindle speed has minimal effect on the angular error of tooth groove wall. When the roll-beating

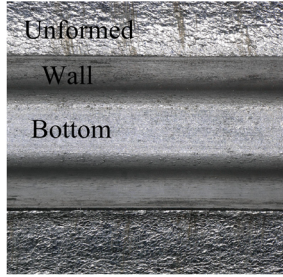
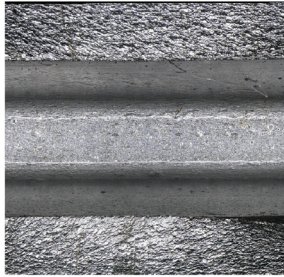
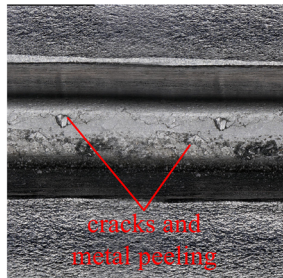
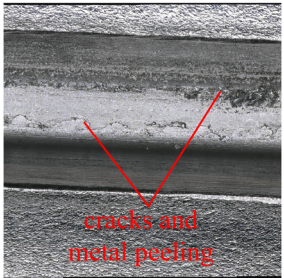
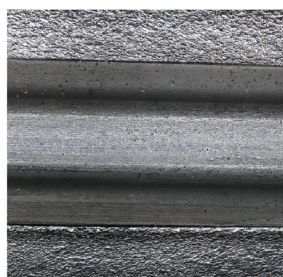

Fig. 18 The effects of process parameters on surface roughness of tooth groove wall: **a** down-beating and **b** up-beating



density is less than 5 mm^{-1} , the error is small at low spindle speeds. When the roll-beating density is greater than 10 mm^{-1} , a high spindle speed is better. The angular error of the tooth groove wall is greatly affected by the roll-beating density. When the roll-beating density is less than 5 mm^{-1} , increasing the roll-beating density causes the angular error of the tooth groove wall to rapidly decrease. The error reaches a minimum when the roll-beating density is $5\text{--}10 \text{ mm}^{-1}$. At this point, continuing to increase the roll-beating density does not help to reduce the error.

For up-beating, the angular error of the tooth groove wall always decreases as the spindle speed increases. At the same spindle speed, when the roll-beating density is less than 5 mm^{-1} , the angular error of the tooth groove wall decreases as the roll-beating density increases, which is due to the rapid decrease in the forming force in this range of roll-beating density. The error caused by the stiffness of the system also decreases. Continuing to increase the roll-beating density causes the error to increase until the roll-beating density exceeds 10 mm^{-1} , at which point the angular error of the tooth

Fig. 19 The surface of tooth groove formed by experiment

Parameter	Down-beating	Up-beating
$w=950 \text{ r/min}$ $w/f=31.67 \text{ mm}^{-1}$		
$w=1500 \text{ r/min}$ $w/f=50 \text{ mm}^{-1}$		
$w=1500 \text{ r/min}$ $w/f=25 \text{ mm}^{-1}$		

groove wall stabilizes at a constant spindle speed. In addition, the angular error of the tooth groove wall during up-beating is slightly higher than during down-beating, which can be observed by comparing Fig. 16a, b.

4.3 Surface morphology

Transmission parts mainly depend on interactions of the tooth groove wall to perform the power transmission. The surface quality of the tooth groove wall directly affects the service life and performance of transmission parts. Observing the surface of the tooth groove wall formed by cold roll-beating, it can be seen that the surface is covered with arc scratches. These scratches are intertwined with one another, and the curvature radius of the arc scratches from the bottom to the top of the tooth groove gradually increases, as shown in Fig. 17.

Based on the forming principle of cold roll-beating, we know that the rolling wheel rotates while roll-beating the workpiece. If the feed motion of the workpiece is ignored for the tooth crest of the rolling wheel, the velocities of rotation and revolution have the same magnitude and opposite direction. Thus, it can be deduced that the surface of the tooth crest of the rolling wheel does not move relative to the formed tooth groove on the bottom surface. However, for a point on the wall of the rolling wheel, because the rotation radius is smaller than the radius of revolution, the velocity of rotation is smaller than that of revolution. Therefore, a point on the wall of the tooth of the rolling wheel moves relative to the wall surface of the formed tooth groove. For points closer to the root of the rolling wheel, the relative tangential motion is larger. Therefore, micro-convexes on the tooth wall of the rolling wheel will scratch the formed tooth groove wall to create an arc scratch. Closer to the top of the formed tooth groove wall, the curvature radius of the arc scratches is larger.

The surface roughness of the tooth groove wall is evaluated by its Sa value. Figure 18 provides the roughness value of the tooth groove wall for different process parameters and shows that cold roll-beating forming can produce better surface quality in the tooth groove wall. The Sa value of the tooth groove wall is less than 0.3 for all selected process parameters. Comparison of the two types of roll-beating methods suggests that the effect of the roll-beating method on the roughness of the formed tooth groove wall is not significant. The surface roughness of the formed tooth groove wall is greatly affected by the spindle speed; the higher the spindle speed is, the worse the surface quality. This is because, with higher spindle speeds, the relative tangential velocity between the rolling wheel wall and the tooth groove wall and the forming force is greater, and the rolling wheel exerts a strong scraping effect on the tooth groove wall. Increasing the roll-beating density causes the frequency of rubbing of the tooth groove wall to increase. Thus, as the roll-beating density increases, the surface roughness increases as well, at least in the lower roll-

beating density range, and attains a maximum when the roll-beating density is in the range of 2~8 mm⁻¹, then, the roll-beating density continues to increase and the surface roughness begins to decrease because the scratches become denser.

A remarkable experimental result was encountered. It was found that, when the spindle speed is 1500 r/min and the roll-beating density is 50 mm⁻¹, cracks and surface metal peeling appear at the bottom of the tooth groove. Below this spindle speed or roll-beating density, the cracks and metal peeling do not occur, as shown in Fig. 19. This result indicates that excessive spindle speeds or roll-beating densities cause the metal deformation of the surface of the bottom of the tooth groove to reach the deformation limit of the material, after which ductile cracks occur.

5 Conclusion

Based on the above results, the following conclusions can be drawn:

- (1) The forming force of down-beating forming is lower than that of up-beating forming. However, for down-beating forming, the direction of the forming force in the feed direction is not consistent. The average maximum forming force perpendicular to the feed direction F_{zm} is less affected by the spindle speed, while the maximum forming force along the feed direction F_{ym} is greatly affected by the spindle speed, both of which increase with increasing spindle speed. F_{zm} decreases as the roll-beating density increases and decreases more rapidly in the region of lower roll-beating density. However, this downward trend is not significant in the regions of higher roll-beating density. F_{ym} initially increases and then decreases as the roll-beating density increases. For up-beating forming, the effect of roll-beating density on F_{ym} is similar to its effect on F_{zm} .
- (2) In the stable forming stage, the compressed metal mainly extends along the tooth groove wall, and the tangential deformation is very small. In the initial stage and the last stage, the tangential plastic deformation is large and causes flash. Flash can be minimized by use of up-beating and lower spindle speeds. To improve the forming precision of the tooth groove angle, using a roll-beating density in the 5~10 mm⁻¹ range and selecting down-beating is more appropriate. If the roll-beating density is greater than 10 mm⁻¹, a higher spindle speed should be used.
- (3) Interlaced arc scratches appear on the surface of the tooth groove wall during cold roll-beating forming. The effect of the roll-beating method on the surface quality of the formed tooth groove wall is not significant. A higher roll-beating density and lower spindle speed are good for

improving the surface quality of the wall of the tooth groove. Excessive spindle speeds or roll-beating densities should be avoided to prevent cracks and surface metal peeling at the bottom of the tooth groove.

Funding information The authors are grateful to National Natural Science Foundation of China (Grant No. 51475366, 51475146), Natural Science Basic Research Plan in Shaanxi Province of China (Grant No. 2016JM5074), and Ph.D. Innovation fund projects of Xi'an University of Technology (Grant No. 310-252071601).

Publisher's Note Springer Nature remains neutral with regard to jurisdictional claims in published maps and institutional affiliations.

References

- Gröbel D, Schulte R, Hildenbrand P, Lechner M, Engel U, Sieczkarek P, Wernicke S, Gies S, Tekkaya AE, Behrens BA, Hübner S, Vucetic M, Koch S, Merklein M (2016) Manufacturing of functional elements by sheet-bulk metal forming processes. *Prod Eng* 10(1):63–80. <https://doi.org/10.1007/s11740-016-0662-y>
- Bauer S (2012) Sustainable materials: with both eyes open. *Mater Today* 15(9):410. [https://doi.org/10.1016/s1369-7021\(12\)70169-4](https://doi.org/10.1016/s1369-7021(12)70169-4)
- Tekkaya AE, Allwood JM, Bariani PF, Bruschi S, Cao J, Gramlich S, Groche P, Hirt G, Ishikawa T, Löbbecke C, Lueg-Althoff J, Merklein M, Misiolek WZ, Pietrzyk M, Shivpuri R, Yanagimoto J (2015) Metal forming beyond shaping: predicting and setting product properties. *CIRP Ann Manuf Technol* 64(2):629–653. <https://doi.org/10.1016/j.cirp.2015.05.001>
- Wang Z (2013) Theory and approach to the less-loading closed die forging. *J Mech Eng* 49(18):92–98. <https://doi.org/10.3901/jme.2013.18.092>
- Yang H, Fan XG, Sun ZC, Guo LG, Zhan M (2013) Some advances in local loading precision forming of large scale integral complex components of titanium alloys. *Mater Res Innov* 15(sup1):s493–s496. <https://doi.org/10.1179/143307511x12858957676119>
- Merklein M, Allwood JM, Behrens BA, Brosius A, Hagenah H, Kuzman K, Mori K, Tekkaya AE, Weckenmann A (2012) Bulk forming of sheet metal. *CIRP Ann Manuf Technol* 61(2):725–745. <https://doi.org/10.1016/j.cirp.2012.05.007>
- Groche P, Fritsche D (2006) Application and modelling of flow forming manufacturing processes for internally geared wheels. *Int J Mach Tools Manuf* 46(11):1261–1265. <https://doi.org/10.1016/j.ijmactools.2006.01.016>
- Wong CC, Danno A, Tong KK, Yong MS (2008) Cold rotary forming of thin-wall component from flat-disc blank. *J Mater Process Technol* 208(1–3):53–62. <https://doi.org/10.1016/j.jmatprotec.2007.12.123>
- Sheu JJ, Yu CH (2007) The cold orbital forging die and process design of a hollow-ring gear part. The 35th International MATADOR Conference, 2007. Springer-Verlag, London, pp 111–114. <https://doi.org/10.1007/978-1-84628-988-0>
- Manfred H, Hubert N, Peter K, Oskar M, Albin G, Hans-Ruedi H (1999) Procedure for manufacture of gearwheel teeth. DE19744639
- Krapfenbauer H (1984) New aspects for the mass production of spur gears by cold rolling. *IPE* 8(3):39–41
- Cui FK, Wang XQ, Zhang FS, Xu HY, Quan JH, Li Y (2013) Metal flowing of in volute spline cold roll-beating forming. *Chin J Mech Eng-En* 26(5):1056–1062. <https://doi.org/10.3901/CJME.2013.05.1056>
- Cui FK, Liu F, Su YX, Ruan XL, Xu SK, Liu LB (2018) Surface performance multiobjective decision of a cold roll-beating spline with the entropy weight ideal point method. *Math Probl Eng* 2018:1–7. <https://doi.org/10.1155/2018/5048387>
- Grob E, Krapfenbauer H (1973) Roller head for cold rolling of splined shafts or gears US3818735
- Cui FK, He XJ, Li Y, Han ZR (2010) Process parameters optimization of ballscrew manufactured by cold rolling. *Appl Mech Mater* 33:268–272. <https://doi.org/10.4028/www.scientific.net/AMM.33.268>
- Li YX, Li Y, Yuan QL (2014) Research on simulation of rack roll-beating forming based on ABAQUS. *J Chem Pharm Res* 6(3):798–805
- Liang XM, Li Y, Cui LM, Yang MS, Xiao JM, Cui FK (2016) The effect of different roll-beating methods on deformation forces of rack cold roll-beating. *Rev Fac Eng* 31(8):164–174. <https://doi.org/10.21311/002.31.8.16>
- Cui FK, He XJ, Li CM, Li Y, Han ZR (2010) Shaping movement analysis and simulation of ballscrew manufactured by cold rolling. *Adv Mater Res* 97-101:4032–4035. <https://doi.org/10.4028/www.scientific.net/AMR.97-101.4032>
- Yang MS, Li Y, Dong H, Li YX (2015) Scale-like texture defect of slab metal cold roll-beating. *Mater Res Innov* 19(sup5):911–915. <https://doi.org/10.1179/1432891714z.0000000001220>
- Ding ZH, Cui FK, Liu YB, Li Y, Xie KG (2017) A model of surface residual stress distribution of cold rolling spline. *Math Probl Eng* 2017:1–21. <https://doi.org/10.1155/2017/2425645>
- Li Y, Li YX, Yang MS, Yuan QL, Cui FK (2015) Analyzing the thermal mechanical coupling of 40Cr cold roll-beating forming process based on the Johnson-cook dynamic constitutive equation. *Heat and Technology* 33(3):51–58. <https://doi.org/10.18280/ijht.330307>
- Kopp R, Wiegels H (1999) Einführung in die Umformtechnik. Verlag Mainz, Aachen
- Groche P, Kramer P (2017) Numerical investigation of the influence of frictional conditions in thread rolling operations with flat dies. *Int J Mater Form* 11(5):687–703. <https://doi.org/10.1007/s12289-017-1383-2>
- Zhang DW, Cui MC, Cao M, Ben NY, Zhao SD (2017) Determination of friction conditions in cold-rolling process of shaft part by using incremental ring compression test. *Int J Adv Manuf Technol* 91(9–12):3823–3831. <https://doi.org/10.1007/s00170-017-0087-6>